https://doi.org/10.70882/8ct1w036

SCIENCE FORUM (JOURNAL OF PURE AND APPLIED SCIENCES) 26, (4) (2026), 251 - 261

Science Forum (Journal of Pure and Applied Sciences)

Journal Homepage: https://atbuscienceforum.com.ng/index.php/jpas

# Hydrothermal Preparation and Optical Characterization of Silver Nanoparticles with Surface Plasmon Resonance Analysis

**Ali Fadhil Abdulaali**

Wasit General Directorate of Education, Wasit, Iraq.

Abstract

In this work, the silver nanoparticles (AgNPs) were synthesized by hydrothermal method and the effect of thermal treatment on structure, morphology and plasmonic properties of the prepared AgNPs were studied. The synthesis process was designed to precisely control the growth of the particles and crystallinity to form nanostructures that can be used for plasmonic applications. The prepared AgNPs were then calcined at 200 °C and 400 °C to check the effect of temperature on the morphology and optical properties of the prepared AgNPs. X-ray diffraction (XRD) and field-emission scanning electron microscopy (FE-SEM) confirmed the formation of a face-centred cubic (FCC) metallic silver phase, with high crystallinity and purity, at 400 °C, where the nanorods had an anisotropic shape with an average diameter of ~7 nm and a length of ~70 nm. The elemental purity and homogeneity of the distribution of Ag in the samples was confirmed by energy-dispersive X-ray spectroscopy (EDX) analysis. The surface plasmon resonance (SPR) feature was seen in the UV–Vis absorption spectra, which is the collective oscillation of the conduction electrons in resonance with the incident absorption light. AgNPs had a well-defined plasmonic absorption peak (~ 410 nm) characteristic of LSPR, being more pronounced for the spherical AgNPs. The nanorod-shaped particles, however, exhibited two plasmonic modes: One transverse mode with a peak around 405 nm (electron oscillations in the direction of the nanrods' length) and a second longitudinal mode with a peak at 850-900 nm (electron oscillations at the cross axis of the nanrods). This resonance splitting and resonance red-shift is spectral evidence of tunable optical response with temperature, which allows a direct correlation between the particle shape, aspect ratio and the plasmonic behavior. The results demonstrate that the hydrothermal synthesis coupled with thermal calcination under controlled conditions is a suitable approach for the tuning of the plasmonic properties of Ag nanostructures. The modulation of SPR observed here has great potential applications in areas such as plasmonic sensing, photocatalytic and optoelectronic applications where the localization of the electromagnetic field and the tunability of the SPR is crucial for high functional performance.

Keywords

Silver Nanoparticles (Agnps);
Hydrothermal Synthesis;
Surface Plasmon Resonance (SPR);
Localized Surface Plasmon Resonance (LSPR)

ISSN 1119-4618 JPAS

Faculty of Science, ATBU Bauchi

Corresponding Author: Ali Fadhil Abdulaali, Wasit General Directorate of Education, Wasit, Iraq. Email: aliaa7648@gmail.com

## 1. Introduction

The unique electronic, optical and catalytic properties of nanoparticles (NPs) and in specially of silver nanoparticles (AgNPs) at the nanoscale have made them a vital area of interest in the field of materials and nanotechnology. These properties are mostly due to their high surface-to-volume ratio and the collective oscillation of the conduction electrons that occurs in the surface known as surface plasmon resonance (SPR) [1-3]. The localized surface plasmon resonance (LSPR), phenomena of intense absorption band in the visible range of electromagnetic spectrum, is due to the oscillation of the conduction electrons in the surface of the nanoparticle when it is hit by electromagnetic waves [4].

The LSPR properties such as the position and intensity of the plasmonic band are very sensitive to the particle size, shape, and surrounding dielectric environment [5, 6] Therefore, among the different synthetic methods, the hydrothermal method has proven to be very efficient for synthesizing AgNPs that have a controlled crystallinity, a uniform shape, and very little surface contamination. This technique allows for the synthesis process parameters to be controlled with accuracy, such as the temperature, pH and concentration of the precursor solution, which directly influence the growth kinetics of the particles as well as the aggregation process [7, 8]. Therefore, hydrothermal synthesis is a way to achieve a controlled tuning of the optical/plasmonic properties of AgNPs that does not require post-synthesis processing.

Optical properties of AgNPs are size-dependent, which play an important role in its plasmonic and sensing properties. As the particle size decreases, the SPR peak moves towards the blue, due to the reduction in the electron mean free path, and the growth in the surface scattering effects [9]. Conversely, bigger nanoparticles also yield higher dipole coupling and retardation effects in the conduction electron cloud that shift the SPR peaks towards the red [9]. Hence, the difference in the size distribution of particles directly affects the sensitivity of the sensors towards gasses based on AgNP. Smaller nanoparticles have more surface energy and more active sites, and have faster and more pronounced responses to the gas adsorbed. Larger particles, however, tend to be less sensitive and less active due to less surface activity [10].

AgNPs give different SPR response in the presence of reducing and oxidizing gases like $H_2S$, $NH_3$, $O_3$ and $NO_2$. It happens due to the change in the local dielectric constant and changes in the electronic structure of the surface of the nanoparticle when gas molecules are adsorbed [11]. Ag–S or Ag–N surface complexes are, for example, created when Ag and sulfur or nitrogen containing gases interact, leading to a decrease in the intensity of the SPR and its shift. Plasmonic gas sensing is based on the changes of the SPR parameters which correspond to the type and concentration of the gas molecule that interacts with the SPR [12, 13].

The correlation between particle size, surface's chemical composition and optical resonance behavior is emphasized, which is essential for the design of plasmonic materials based on AgNP in the controlled synthesis. In the present study, the hydrothermal method is used to synthesize the AgNPs and characterize the same using

optical characterization with a particular emphasis on the study of the behaviour of surface plasmon resonance. An SPR response–particle size distribution relationship has been established and this work opens the door to getting a better understanding of the plasmonic sensitivity mechanisms of Ag nanoparticles and their potential use in environmental monitoring and detection of gases.

**Experimental Procedures**

**Materials**

All reagents used in this study were analytical grade, and were used without further purification. Silver nitrate (Silver nitrate, $AgNO_3$, ≥99.9%, Sigma-Aldrich) was used as a silver precursor and sodium hydroxide (Sodium hydroxide, NaOH, ≥98%, Merck) was used as a pH adjusting agent. De-ionized (DI) water was used throughout the synthesis process to remove the presence of the ionic impurities that could affect the growth of the nanoparticles and/or the optical properties. All glassware were washed in nitric acid and then rinsed with DI water to decontaminate the glassware.

**Hydrothermal Synthesis of Silver Nanoparticles**

A hydrothermal synthesis procedure was used to prepare the silver nanoparticles (AgNPs) in a way that allowed for controlled thermodynamic conditions and uniform nucleation and particle growth. AgNO3 (0.01 M) and NaOH (0.02 M) were prepared separately and mixed on magnetic stirrer at room temperature. The pH of the solution was slowly increased to approximately 10 by dropwise addition of the NaOH solution, and the precursor solution was $AgNO_3$ so that it can form favourable Ag+ complexes that can be used to nucleate nanoparticles.

The colloidal mixture was then placed into a Teflon lined stainless-steel autoclave (100 mL capacity) and heated at 180 °C for 6 hours in a programmable oven. The silver ions were reduced in the small volume under the hydrothermal condition, and silver nuclei grew. The collected precipitate was then centrifuged at 8000 rpm for 10 minutes and washed with ethanol and DI water several times to wash away the unreacted species and then dried in an air oven at 60 °C for 12 hours. The resultant AgNP powder was further ground gently and kept in air-tight containers for further characterization.

**The production of thin films of silver**

The cleaned slides were then placed into the Teflon liner, vertically, in a custom-made Teflon rack so as to prevent them from coming in contact with the walls of the liner before the sealing. The reaction mixture of $AgNO_3$ and NaOH (as described above) was poured into the liner and the substrates were completely covered. The autoclave was then kept at 180 °C for 6 h. During the reaction, a uniform thin film of uniform size of the silver nanoparticles was obtained by heterogeneous nucleation and growth process on the glass surface.

Once the coated substrates were cooled down, they were gently washed with DI water prior to being dried at 50 °C for 2 hours. The resultant thin Ag films were metallic gray in colour and had a uniform reflective surface. These films were employed for optical and surface analysis and compared to the plasmonic response of the colloidal AgNPs. When a thin silver film is deposited at

different temperatures, two thin silver films are formed.

**Preparation of Two Thin Silver Films at Different Temperatures**

The two samples were prepared by the hydrothermal deposition technique and were then thermally treated at various temperatures to study the effect of thermal treatment on the structure and optical properties of the silver thin films. The synthesis up to thermal treatment step was identical to ensure the same chemical composition and precursor concentration of both films.

**Silver films can be deposited by hydrothermal processes**

To investigate the effects of thermal energy on the nucleation kinetics, crystal growth and surface morphology, 2 thin silver films were prepared using the hydrothermal deposition method at different reaction temperature, one at 200 °C and the other at 400 °C. Cleaned glass substrate (1 × 2 cm) has been used as a glass substrate for deposition. The substrates were ultrasonically washed for 10 min in acetone, ethanol and deionized (DI) water then dried by blowing with nitrogen to eliminate the moisture and organics.

The precursor solution was $AgNO_3$ (0.01 M) in DI water and sodium hydroxide (NaOH, 0.02 M) was then added dropwise to the precursor solution under magnetic stirring until the final pH was reached (around 10). The alkaline environment allowed for the creation of complexes of silver–hydroxide which were then reduced to metallic silver in the hydrothermal process. This prepared solution was transferred to a Teflon-lined stainless-steel autoclave (100 mL. capacity). The glass surfaces of cleaned glass substrates were not in contact with the walls of the autoclave, but were supported on a vertical non-reactive Teflon rack to ensure they were all in contact with the reactive medium.

The autoclave was closed and heated to 200 °C for 6 h in a programmable oven, to heat the first thin film (Ag–200 °C). Under these conditions, moderate thermal energy led to the formation of more nuclei, and the growth rate was decelerated, which led to the formation of a fine-grained coating of silver nanoparticles.

To obtain the second thin film (Ag–400 °C), the hydrothermal process was repeated at 400 °C for 6 h. A higher temperature provided more diffusion energy to the silver atoms and thus more crystals were coalesced, producing more crystalline, larger and silver nanoparticles on the surface.

The autoclaves were naturally cooled to room temperature after both syntheses. The coated glass slides were washed gently a few times with DI water to remove the loosely bound particles and then dried in the air oven at 50 °C for 2 h.

The resulting silver films had metallic grey-colored surfaces and smooth and continuous surfaces. Interestingly, the Ag–400 °C film was slightly darker and more reflective than the Ag–200 °C film, indicating greater grain growth in this film, and better ordering of surface atoms than in the Ag–200 °C film. Different behaviours of the synthesized nanostructures are a clear example of the strong temperature dependence of the physicochemical evolution of the synthesized silver nanostructures in hydrothermal growth.

**The study of calcination of thin films of silver**

Two hydrothermally prepared Ag thin films were annealed (calcined) at various temperatures to study the effect of thermal treatment on morphology, crystallinity and optical response: The thin films were calcined for 2 hours in air at 400 °C. This increase in temperature led to better grain coalescence and increase in particle size and crystallinity; the surface roughness and reflectivity may have changed as well. The two samples were gradually removed from the hot furnace to the ambient temperature to prevent any cracking due to thermal stresses. Thus, obtained films were kept in the desiccators for subsequent optical characterization.

## 3. Results and Discussion

### 3.1 Structural Analyses (XRD, EDX, SEM) of Ag thin films

The X-ray diffraction (XRD) pattern of the silver nanoparticles prepared by hydrothermal method and then calcined at 200 °C is shown in Figure 1. The diffraction peaks are indexed as FCC (face-centered cubic) crystal structure of metallic silver (as per the COD reference card No. 96-900-8460). The characteristic reflections appear at 2θ = 39.11°, 44.55°, 62.01°, and 65.88°, which correspond to the crystallographic planes (111), (200), (202), and (311), respectively. The high crystallinity and phase purity of the synthesized material is confirmed by the sharp and well-defined peaks. No extra or spurious diffraction peak exists, which suggests no secondary phases or impurities are present and means that the sample is predominantly made up of pure metallic silver. The most intense reflection in comparison with the other reflections which appeared at 39.11° diffraction is the (111) reflection, which is also the most preferred growth direction for the Ag nanoparticles as it has the lowest surface energy configuration of FCC metallic nanostructures.

The diffraction peaks have a narrow FWHM which is further evidence of well-developed crystallites with low lattice strain. The average crystallite size (d) can be obtained from the FWHM of the (111) reflection using the Debye- Scherrer equation, and is inversely proportional to the FWHM, which means more coherent scattering domain. The relation is important for obtaining information on the amount and the nanocrystalline size of the order of the material. All these facts support the highly crystalline FCC nanoparticles of Ag metal that are obtained by the hydrothermal process and calcination process at 200 °C [14].

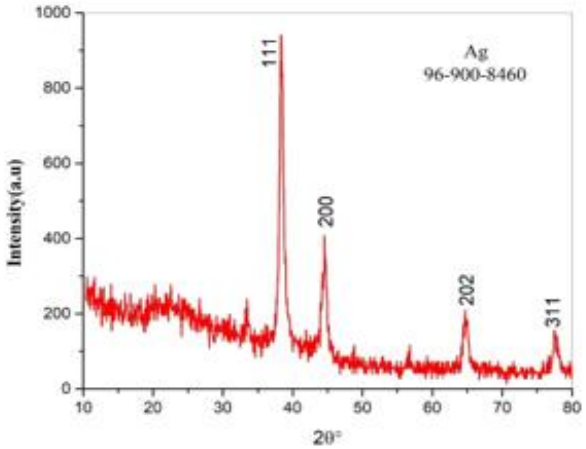


Figure 1. XRD diffraction pattern of hydrothermally synthesized Ag nanoparticles after calcination at 200°C, showing the characteristic reflections of crystalline FCC silver.

The sizes of the average crystal of Ag, Cu and Ag-Cu were calculated by the Scherrer equation [15,16].

$$D = \frac{K\lambda}{\beta COS\theta}$$

The shape factor, K, is equal to 0.945, Full width at half maximum (FWHM), is equal to 0.179, X-ray wavelength (λ) is equal to 0.16516 nm.

The data shown in the Energy-Dispersive X-ray (EDX) spectrum in Figure 2 further confirms the elemental composition of the synthesized nanomaterial. The analysis shows very sharp and strong peaks corresponding to the silver (Ag) confirming the formation of a pure metallic silver nanoparticle.

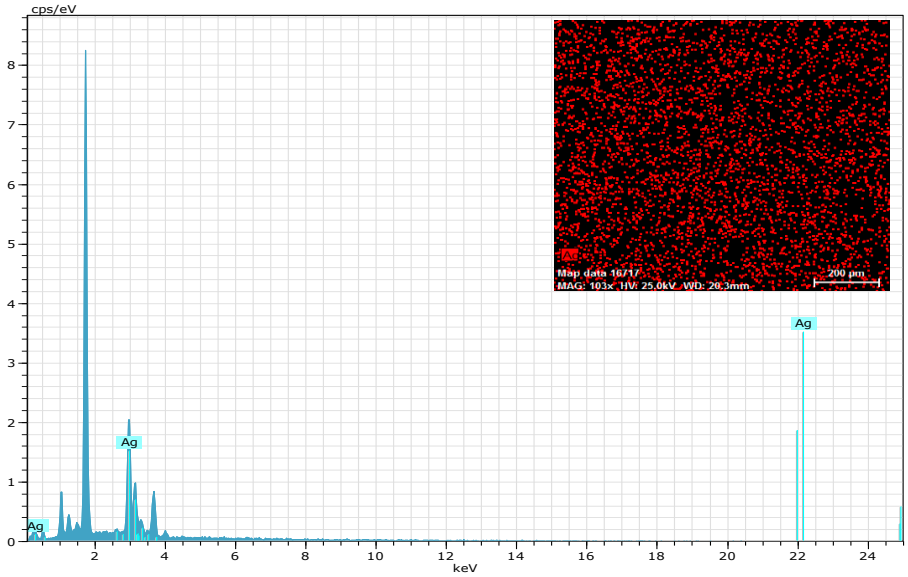


Figure 2. EDX spectrum and elemental distribution map of Ag nanoparticles synthesized by the hydrothermal method and calcined at 400 °C.

The highest peaks in the Ag ones are at ~ 3 keV (Ag La line) and at ~ 22 keV (Ag Ka line), which are the energies of the transition of electrons in the Ag atomic orbits. The intensity of these peaks indicates that the prepared nanoparticles are made up of silver atoms and that there is not much contamination in the prepared nanoparticles and/or secondary phases. No other elements (C, O, Cl, etc.) are significant, meaning that the product is quite pure and that the precursor compounds from the hydrothermal synthesis process are not particularly present in the product. In plasmonic and catalytic applications, such purity is vital for uniform electronic and optical properties when using the device. The inset EDX elemental mapping image also supports this conclusion, with equal distribution of Ag atoms in the entire area of the sample. The uniformity of the colour of the mapped area indicates the uniform distribution of the silver nanoparticles in the area without any significant clustering or compositional variation between the nanoparticles.

The quantitative EDX analysis showed that only silver (Ag) element is detected and the weight percentage and atomic percentage of silver is 100% and 100% respectively. The results obtained are in agreement with the excellent purity of the hydrothermally synthesized Ag nanoparticles after the calcination treatment at 200 °C and suggest that there is no detectable impurities and

secondary phases in the nanoparticles in the range of the EDX detection limit.

With the powerful ability of directly imaging the surface architecture, size distribution and morphology of nanoparticles with high spatial resolution, the Scanning Electron Microscope (SEM) is one of the most powerful and widely used instruments for the characterization of nanomaterials. The hydrothermal method was used to synthesize the silver (Ag) nanoparticles followed by their characterization in this study using Field Emission Scanning Electron Microscopy (FE-SEM), which has led to detailed information about the nano-architecture of the synthesized silver nanoparticles [1,11,13-16].

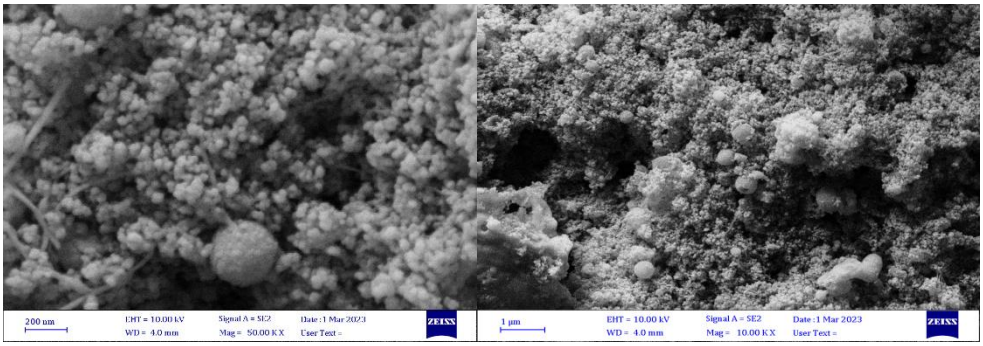


Figure 3. FE-SEM images of spherical Ag nanoparticles obtained after calcination at 200 °C.

Figure 3 shows the FE-SEM image of the sample after calcination at 200 °C that displays aggregated nanoparticles with a relatively uniform grain-size distribution. The small surface morphology indicates that fine nanostructural features are maintained because of the lower calcination temperature, which did not allow for overt grain growth and coalescence. This morphology can give a relatively high surface area, which is beneficial for catalytic and sensing applications because of increased number of active surface sites that can interact with the surrounding species, [7, 8, 11, 13-16].

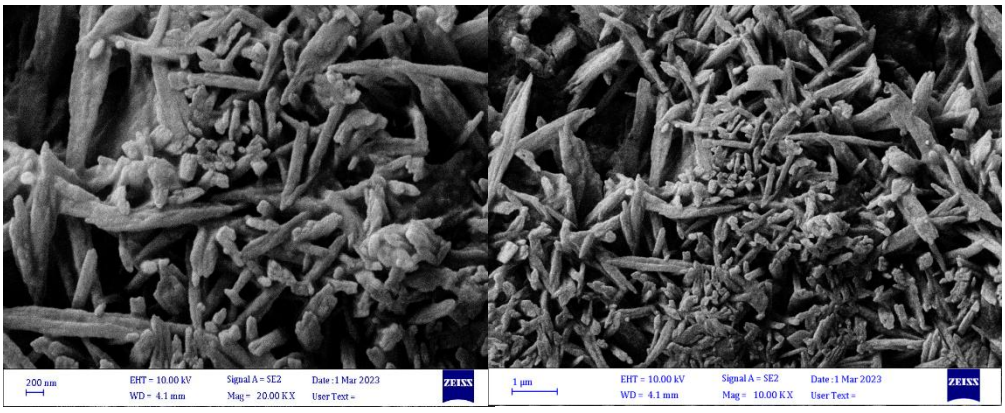


Figure 4. FE-SEM images of Ag nanorods formed after calcination at 200 °C, illustrating temperature-induced anisotropic crystal growth.

The FE-SEM micrograph, made at 200 °C (Figure 4), shows that the silver nanoparticles are one dimensional, having a rod-like morphology, indicating anisotropic crystal growth at higher calcination temperatures. The average length of the nanorods observed was approximately 70 nm and the diameter was approximately 7 nm, which shows a high aspect ratio, characteristic of directing the crystal growth along crystallographic planes.

The growth of the Ag nuclei probably takes place along the thermodynamically more favourable crystal directions [110] or [111] in hydrothermal environment, which accounts for this elongated rod-like shape. Such high temperatures enable better surface diffusion and atomic mobility which results in the grain merging to form elongated nanowire structures. This kind of thermal activation lowers the surface energy by decreasing the total count of high-energy facets which makes the system go towards an energetically more stable rod-shaped configuration.

From a material science lens, the formation of this anisotropic structure also allows the exposure of the crystallographic faces from the material, which can significantly influence optical, catalytic and electronic properties of the silver nanoparticles. These nanorods have sharp edges and elongated shapes which are beneficial for plasmonic resonance enhancement and electron transport, and are thus potential candidates for various photonic, catalytic and sensing applications. The formation of well-defined rods at 200 °C, therefore, suggests that temperature is an important parameter controlling the shape evolution of the synthesized Ag nanostructures from quasi-spherical aggregates at low temperature to elongated rods at high thermal conditions [1,5,8,13-16].

### 3.2 UV-VIS Plasmon resonance Absorption spectra Analyses of Ag

A UV-Vis spectrometry was used to study the surface plasmonic properties of the synthesized silver nanoparticles (AgNPs) in a wavelength range of 0 nm to 1100 nm. One of the most remarkable optical characteristics of noble metal nanoparticles, especially silver, is Surface Plasmon Resonance (SPR), the collective oscillation of conduction-band electrons, caused by the incident electromagnetic radiation. The plasmonic band with the highest absorbance was observed at ~410 nm, typical of quasi-spherical AgNPs.

This absorption band is created by coherent oscillation of free electrons at the surface of the nanoparticle whose Coulombic restoring force between the displaced electron cloud and the positive charge of the metal lattice creates a resonance at a certain optical frequency. The SPR band observed supports the successful synthesis of silver nanoparticles exhibiting well-defined plasmonic properties and also provides useful information with regard to size, shape and dispersion state of the nanoparticles [1,5,9,13-16].

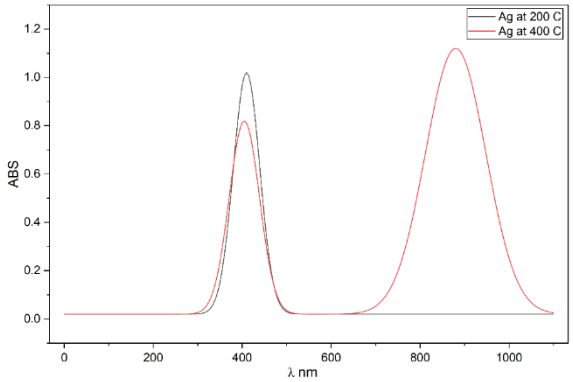


Figure 5. UV-Vis absorption spectra of Ag nanostructures calcined at different temperatures, showing the transition from localized surface plasmon resonance (LSPR) to dual plasmonic modes associated with nanorod formation.

The position and shape of this plasmon peak in Fig. 5 are very sensitive to the size, shape, dielectric environment and aggregation of the particles. The resonance of quasi-spherical AgNPs in the range of 20-40 nm is typically in the 400-430 nm range. The symmetrical peak in this range is further evidence of the formation of well-dispersed silver nanoparticles with little agglomeration and uniform morphology. When the nanoparticles change from being spherical to being anisotropic nanorods, the optical spectrum changes to include two resonant modes: A transverse mode around ~405 nm corresponding to oscillations of the electrons transverse to the axis of the rod. A mode that shows up in the near-infrared range (~850-900 nm) that corresponds to the oscillations of the electrons along the long axis of the nanorods.

The shape and aspect ratio (length/diameter ≈ 10) causes this spectral splitting, and the change of aspect ratio of the container causes a red shift to the longitudinal resonance, due to the reduction in the restoring force along the long axis. Thermal treatment at 400 °C leads to a broadened and red-shifted overall absorbance profile, thus corroborating the isotropic (spherical) to anisotropic (rod-like) transition of the nanostructures. The dual plasmon bands further enhance the plasmonic sensing, photothermal conversion and nonlinear optical applications of the material where the near surface phenomena are highly enhanced by the localized electromagnetic fields at the resonance [1,5,9,12,13-16].

**Conclusion**

The hydrothermal method was successfully used to synthesize silver nanoparticles (AgNPs) and systematically characterized to investigate the correlation of structural morphology of the nanoparticles with surface plasmon resonance (SPR) behavior. The XRD, FE-SEM and EDX analyses revealed the highly crystalline and phase-pure nanoparticles of metallic silver with face-centered cubic (FCC) structure. The calcination temperature was found to play an important role on the particle morphology and the optical properties.

The AgNPs showed the highest quality of quasi-spherical particles, and possessed a relatively narrow particle size distribution when calcined at 200 °C, while the 400 °C calcination led to the growth of one-

dimensional nanorods with an average length of ~70 nm and an average diameter of ~7 nm. Using the UV–Vis optical analysis, the temperature-dependent and well-resolved SPR features were observed. The quasi-spherical nanoparticles showed only one plasmonic band at 410 nm, a typical feature of the dipolar localized surface plasmon resonance (LSPR) of small isotropic (spherical) silver nanoparticles. The spectrum was transformed into elongated nanorods at 400 °C, with the appearance of two resonances: one in the transverse mode at ~405 nm and a second in the longitudinal mode in the near IR region (850-900 nm).

This split on the spectral scale is a direct proof of the anisotropy of the electron oscillation inside the rod-like nanostructure, and it also verifies the possibility of successful tuning of the plasmonic response of such nanostructures by thermal treatment. The results show that hydrothermal synthesis and thermal modulation is a very simple and effective way of controlling the plasmonic and optical properties of silver nanoparticles. The localization of the field and the dual-band plasmonic resonance in the nanorod structures are extremely interesting for applications like plasmonic sensing,

photocatalytic, and photothermal applications. The correlation between the morphological anisotropy and the SPR response, developed in this work, is helpful in developing fundamental understanding of the structure–property relations in noble-metal nanostructures and is a scalable approach for engineering more advanced plasmonic materials for environmental applications and for optoelectronic devices.

**References**


[1] U. Kreibig and M. Vollmer, *Optical properties of metal clusters*. Springer Science & Business Media, 2013.

[2] S. Link and M. A. J. T. J. o. P. C. B. El-Sayed, "Size and temperature dependence of the plasmon absorption of colloidal gold nanoparticles," vol. 103, no. 21, pp. 4212-4217, 1999.

[3] H. J. Hassan and A. Y. J. J. T. Alam, "Synthesis And Characterization of Magnesium Oxide-Doped Iron (Iii) Oxide Nanoparticles by Sol-Gel Method," vol. 87, no. 5, pp. 907-914, 2025.

[4] J. N. Anker, W. P. Hall, O. Lyandres, N. C. Shah, J. Zhao, and R. P. J. N. m. Van Duyne, "Biosensing with plasmonic nanosensors," vol. 7, no. 6, pp. 442-453, 2008.

[5] C. F. Bohren and D. R. Huffman, *Absorption and scattering of light by small particles*. John Wiley & Sons, 2008.

[6] S. Pillai, K. Catchpole, T. Trupke, and M. J. J. o. a. p. Green, "Surface plasmon enhanced silicon solar cells," vol. 101, no. 9, 2007.

[7] S. J. G. c. Iravani, "Green synthesis of metal nanoparticles using plants," vol. 13, no. 10, pp. 2638-2650, 2011.

[8] Y. Sun and Y. J. s. Xia, "Shape-controlled synthesis of gold and silver nanoparticles," vol. 298, no. 5601, pp. 2176-2179, 2002.

[9] P. J. L. Mulvaney, "Surface plasmon spectroscopy of nanosized metal particles," vol. 12, no. 3, pp. 788-800, 1996.

[10] V. Amendola and M. J. T. J. o. P. C. C. Meneghetti, "Size evaluation of gold nanoparticles by UV– vis spectroscopy," vol. 113, no. 11, pp. 4277-4285, 2009.

[11] A. J. T. J. o. P. C. Henglein, "Physicochemical properties of small metal particles in solution:" microelectrode" reactions, chemisorption, composite metal particles, and the atom-to-metal transition," vol. 97, no. 21, pp. 5457-5471, 1993.

[12] O. A. Yeshchenko, I. M. Dmitruk, A. A. Alexeenko, A. V. Kotko, J. Verdal, and A. O. J. P. Pinchuk, "Size and temperature effects on the surface plasmon resonance in silver nanoparticles," vol. 7, no. 4, pp. 685-694, 2012.

[13] K.-S. Lee and M. A. J. T. j. o. p. c. B. El-Sayed, "Gold and silver nanoparticles in sensing and imaging: sensitivity of plasmon response to size, shape, and metal composition," vol. 110, no. 39, pp. 19220-19225, 2006.

[14] A. N. Tuama, "Thermally deposited silver-doped cuprous oxide solar cell on textured silicon and its devices modelling," Universiti Tun Hussein Onn Malaysia, 2022.

[15] M. Miranda and J. J. F. o. C. Sasaki, "The limit of application of the Scherrer equation," vol. 74, no. 1, pp. 54-65, 2018.

[16] U. Holzwarth and N. J. N. n. Gibson, "The Scherrer equation versus the'Debye-Scherrer equation'," vol. 6, no. 9, pp. 534-534, 2011.